INL/CON-13-28386
PREPRINT

SiC-CMC-Zircaloy-4 Nuclear Fuel Cladding Performance During 4-Point Tubular Bend Testing

LWR Fuel Performance Meeting/Top Fuel 2013

I. J. van Rooyen
W. R. Lloyd
T. L. Trowbridge
S. R. Novascone
K. J. Wendt
S. M. Bragg-Sitton

September 2013

Idaho National Laboratory

SIC-CMC-ZIRCALOY-4 NUCLEAR FUEL CLADDING PERFORMANCE DURING 4-POINT TUBULAR BEND TESTING

IJ van Rooyen, W R Lloyd, T L Trowbridge, S R Novascone, K M Wendt, S M Bragg-Sitton*
Idaho National Laboratory, Idaho Falls, ID 83415-6188, USA

KEYWORDS:
SiC-CMC sleeves, Tubular bend test,

* Corresponding author. Tel +1208 526 4199
E-mail address: Isabella.vanRooyen@inl.gov

The U.S. Department of Energy Office of Nuclear Energy (DOE NE) established the Light Water Reactor Sustainability (LWRS) program to develop technologies and other solutions to improve the reliability, sustain the safety, and extend the life of current reactors. The Advanced LWR Nuclear Fuel Development Pathway in the LWRS program encompasses strategic research focused on improving reactor core economics and safety margins through the development of an advanced fuel cladding system. Recent investigations of potential options for "accident tolerant" nuclear fuel systems point to the potential benefits of silicon carbide (SiC) cladding. One of the proposed SiC-based fuel cladding designs being investigated incorporates a SiC ceramic matrix composite (CMC) as a structural material supplementing an internal Zircaloy-4 (Zr-4) liner tube, referred to as the hybrid clad design. Characterization of the advanced cladding designs will include a number of out-of-pile (nonnuclear) tests, followed by in-pile irradiation testing of the most promising designs. One of the out-of-pile characterization tests provides measurement of the mechanical properties of the cladding tube using four point bend testing. Although the material properties of the different subsystems (materials) will be determined separately, in this paper we present results of 4-point bending tests performed on fully assembled hybrid cladding tube mock-ups, an assembled Zr-4 cladding tube mock-up as a standard and initial testing results on bare SiC-CMC sleeves to assist in defining design parameters. The hybrid mock-up samples incorporated SiC-CMC sleeves fabricated with 7 polymer impregnation and pyrolysis (PIP) cycles. To provide comparative information; both 1- and 2-ply braided SiC-CMC sleeves were used in this development study. Preliminary stress simulations were performed using the BISON nuclear fuel performance code to show the stress distribution differences for varying lengths between loading points and clad configurations. The 2-ply sleeve samples show a higher bend momentum compared to those of the 1-ply sleeve samples. This is applicable to both the hybrid mock-up and bare SiC-CMC sleeve samples. Comparatively both the 1- and 2-ply hybrid mock-up samples showed a higher bend stiffness and strength compared with the standard Zr-4 mock-up sample. The characterization of the hybrid mock-up samples showed signs of distress and preliminary signs of fraying at the protective Zr-4 sleeve areas for the 1-ply SiC-CMC sleeve. In addition, the microstructure of the SiC matrix near the cracks at the region of highest compressive bending strain shows significant cracking and flaking. The 2-ply SiC-CMC sleeve samples showed a more bonded, cohesive SiC matrix structure. This cracking and fraying causes concern for increased fretting during the actual use of the design. Tomography was proven as a successful tool to identify open porosity during pre-test characterization. Although there is currently insufficient data to make conclusive statements regarding the overall merit of the hybrid cladding design, preliminary characterization of this novel design has been demonstrated.

I. INTRODUCTION

The U.S. Department of Energy Office of Nuclear Energy (DOE NE) established the Light Water Reactor Sustainability (LWRS) program to develop technologies and other solutions to improve the reliability, sustain the safety, and extend the life of current reactors. The Advanced LWR Nuclear Fuel Development Pathway in the LWRS program encompasses strategic research focused on improving reactor core economics and safety margins through the development of an advanced fuel cladding system. Recent investigations of potential options for “accident tolerant” nuclear fuel systems point to the potential benefits of silicon carbide (SiC) cladding.

One of the proposed SiC-based fuel cladding designs being investigated incorporates a SiC ceramic matrix composite (CMC) as a structural material supplementing an internal Zircaloy-4 (Zr-4) liner tube, referred to as the hybrid clad design (Fig. 1).

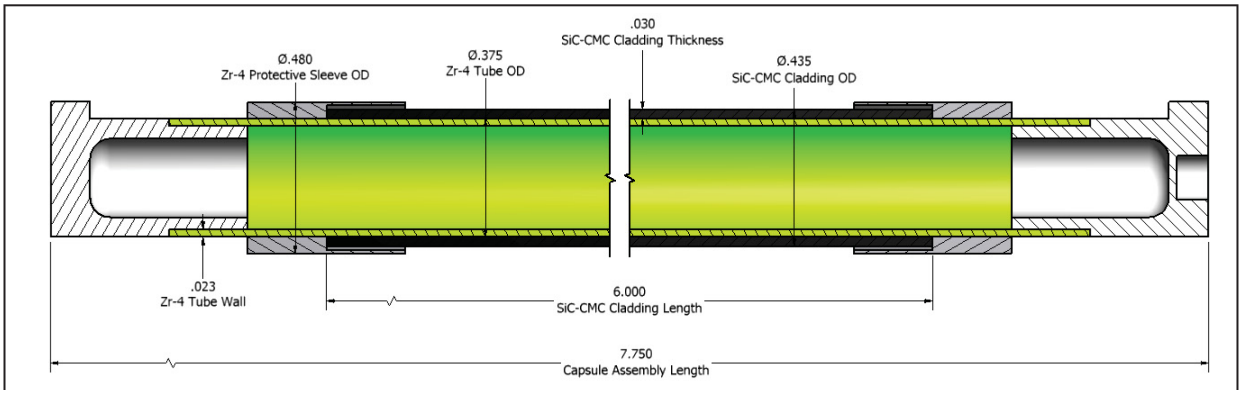

Fig.1. Geometry of the LWRS capsule assembly design for the Si-CMC hybrid Zr-4 cladding rodlet (Ref. 1).

Characterization of the advanced cladding designs will include a number of out-of-pile (nonnuclear) tests, followed by in-pile irradiation testing of the most promising designs. One of the out-of-pile characterization tests provides measurement of the mechanical properties of the cladding tube using four point bend testing. Although the material properties of the different subsystems (materials) will be determined separately, in this paper we present results of 4-point bending tests performed on fully assembled hybrid cladding tube mock-ups, an assembled Zr-4 cladding tube mock-up as a standard and initial testing results on bare SiC-CMC sleeves to assist in defining design parameters. The hybrid mock-up samples incorporated SiC-CMC sleeves fabricated with 7 polymer impregnation and pyrolysis (PIP) cycles (See (Ref. 3) for more detail on the basic properties of the SiC-CMC sleeves). To provide comparative information both 1- and 2-ply braided SiC-CMC sleeves were used in this development study.

II. METHOD DEVELOPMENT

Four-point bending tests were performed on fully assembled hybrid cladding tube mock-ups, an assembled Zr-4 cladding tube mock-up as a standard and initial testing results on the bare SiC-CMC sleeves. It was also important for this program that the actual surface finish of the SiC-CMC sleeve is used during this test and no specimen preparation is used to obtain a smooth defect free surface. Typically for four point bend tests, a support span-to-loading span ratio of either 3:1 or 4:1 can be used. This ratio is shown schematically in Fig. 2.

The nuclear fuel performance code BISON (Ref. 2) was used to perform some preliminary simulations of the 4-point bend tests. The simplifying assumptions of clamped support conditions (no rotations allowed at the supports), an arbitrary prescribed displacement, and elastic properties of Zr-4 were used for the preliminary calculations. The simulation results were not used to guide the experiment approach; the intent of the simulation was to gain some understanding of the effective stress distributions between the two proposed support locations (3:1 vs. 4:1) and to show a preliminary result from this emerging simulation tool (Fig. 3). Future work is planned for more realistic simulations that make use of the large displacement, nonlinear material models, and mechanical contact capabilities that are available in BISON and will hopefully have an influence on experiment design and interpretation of results. It was decided to proceed with the initial method development using a 3:1 span width ratio for the four point bend tests.

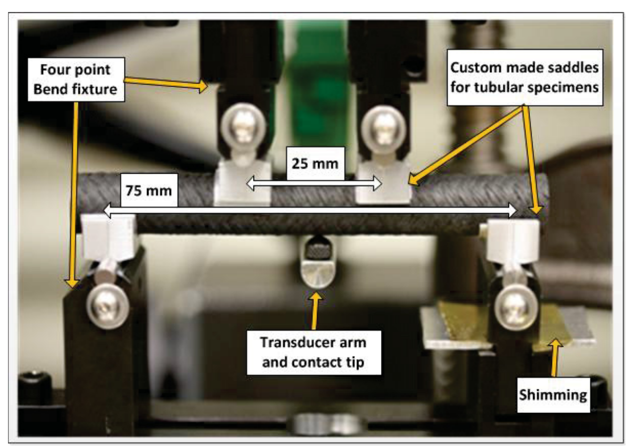

Fig. 2. Photograph demonstrating the 3:1 span width ratio determination and bend test parts. Shims were used to lock the articulated support, since the round specimen did not provide constraint against support roller rotation (as a flat-bottom specimen would).

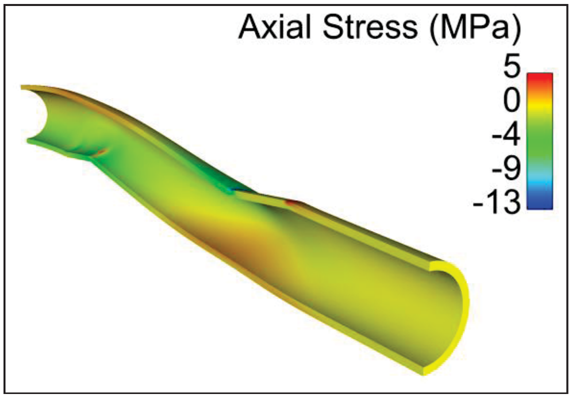

Fig. 3. Initial simulation results presenting the elastic case during a four point bend test with a 3:1 load span width on Zr-4. The simulation was completed on half of the specimen length.

An Instron 5984 test machine and a 5 kN load cell was used. The load cell is calibrated to NIST-traceable force reference standards annually by the INL Standards & Calibration Laboratory. Specimen mid-span deflection was measured with a deflectometer mounted to the bend fixture base. The deflectometer is calibrated daily, before use, with a NIST-traceable displacement calibration stand. The specimen tests and data acquisition are controlled via an attached computer running Instron Bluehill 3 software (v.3.13.1260), and a test “method” control file that controls all aspects of the progress of the test and data acquisition and logging.

A commercial, articulated four-point bend (4PB) test fixture was used for the tests. Normally, these fixtures use line contact rollers, as typical bend specimens have flat surfaces. To avoid localized damage at the point contact where a roller would contact a cylindrical specimen at right angles, support saddles for the round specimen cross-section were fabricated by INL as shown in Fig. 4. The saddles distributed the contact forces over about 135 deg. of specimen circumference, and about 9.5 mm of specimen length. These saddles prevent local damage to the specimens, especially the SiC composite tubes, by distributing the contact force over a relatively large area. Curved saddle liner shims were fabricated to match the saddle support radius to each specimen radius to provide a uniform contact area. To prevent axial constraint as the specimens deformed during testing, and to maintain controlled fixture geometry, the saddles included a radiused contact that matched the fixture roller radius. During the tests, the saddles are free to rotate with the specimen surface, maintaining uniform contact with the specimen surface.

For the plain SiC composite sleeves tested, support cylinders were fabricated from acetyl material. These cylinders were made to closely fit the inside diameter of the test specimen tubes (Fig. 4). The cylinders were located precisely within the tube to correspond to the saddle contact areas on the outside of the tube. The intent of this configuration was to prevent localized stress or strain concentrations near the support contacts, and induce specimen damage accumulation in the central, unsupported, constant bending moment area. Post-test observation of specimen damage suggests the approach was successful.

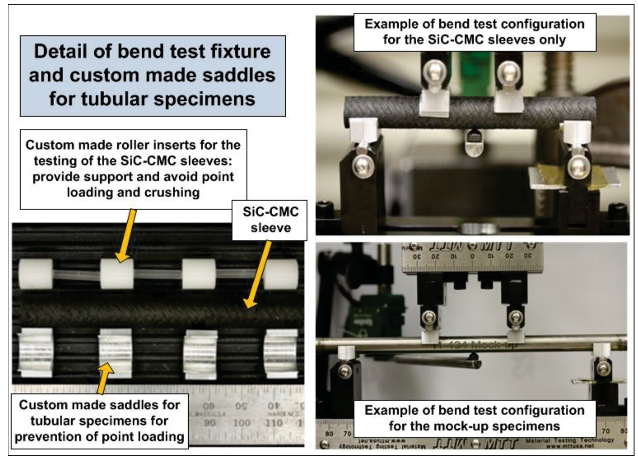

Fig. 4. Bend test fixture and saddle design for the mock-up specimens and SiC-CMC sleeves.

III. BEND TEST RESULTS

Initial testing started with the Zr-4 mock-up tube (SiC-6) to verify that the bend fixture, support saddles, and test control program were sufficient. A strain rate of 1.0 mm/min was initially used for the Zr-4 mock-up specimen. The strain rate was decreased to 0.5 mm/min for the hybrid mock-up specimens as it was unknown at that stage how soon changes will be noted. The strain rate was further decreased during the bend test method development for the SiC-CMC sleeves. The strain rates were chosen to be on the order of 0.1 to 0.25% /min which are regular tensile test strain rates. At these low rates no rate effects of consequence were expected. A summary of the bend test process parameters is provided in Table 1.

Table 1. Bend test process parameters for all specimens tested during method development.

Specimen number	Specimen Description	Load Point Displacement rate (mm/min)	Span widths (S1/S2) (mm)	S1/S2 ratio
LWRS-1-6-A-2-3	5 cycles, 2-ply Sleeve only	0.15	75/25	3:1
LWRS-1-6-A-3-4	5 cycles, 1-ply Sleeve only	0.25*	75/25	3:1
LWRS-1-6-A-6	5 cycles, 1-ply Sleeve only	0.15	75/25	3:1
LWRS-1-6-A-9 (SiC-1)	7 cycles, 2-ply Hybrid	0.5	120/40	3:1
LWRS-5-6-B-1 (SiC-2)	7 cycles, 1-ply Hybrid	0.5	120/40	3:1
SiC-6	N/A Zr-4 assembled	1.0	140/46.7	3:1

*First bend test on SiC-CMC sleeves. The strain rate was found to be too fast and was decreased for the next two tests.

III.A. Mock-up Hybrid Specimens

The first test on the Zr-4 mockup tube showed a shortfall in the initial test, as a maximum deflection value of 10% prohibited the test to continue to a maximum load condition for Zr-4 as shown in Fig. 5. This was corrected when the hybrid mock-up specimens were conducted. The deflectometer used in the test, shown in Fig. 6, provided a more accurate measurement of the deflection up to 2% changes, as it was important to detect early material changes. Additionally, the deflectometer provided verification for the built-in deflection measurement system (crosshead displacement encoder) of the Instron test machine. (Graphs in Fig. 5 show only the Instron measurements).

The bend test at the start and completion of all three mock-up specimens are shown in Fig. 6 to Fig. 8. The support saddles and liner shims moved relative the specimen surface during testing of SiC-1 and SiC-2 specimens. This is due to the relative rotation of the specimen and saddles, and the distance between the bend fixture contact points and specimen centerline. There will be some influence on the actual applied bend moment due to this geometry change, but it was equivalent for both SiC specimens, so the relative difference in mechanical response between SiC-1 and SiC-2 is still representative of true behavior. The plain Zr-4 tube was tested with a slightly longer support span, but S1/S2 was maintained at 3. It is seen from Fig. 5, that the 2 ply SiC-CMC hybrid mock-up specimen exhibited the highest bending stiffness, while the plain Zr-4 tube specimen exhibited the lowest. Cracking and buckling of the SiC-CMC fibers were observed for the 2-ply braided sleeve hybrid mock-up specimen (SiC-1) in the region of highest (nominally constant) compressive bend stress, while no buckling or cracking was observed for the 1-ply braided hybrid mock-up specimen (SiC-2).

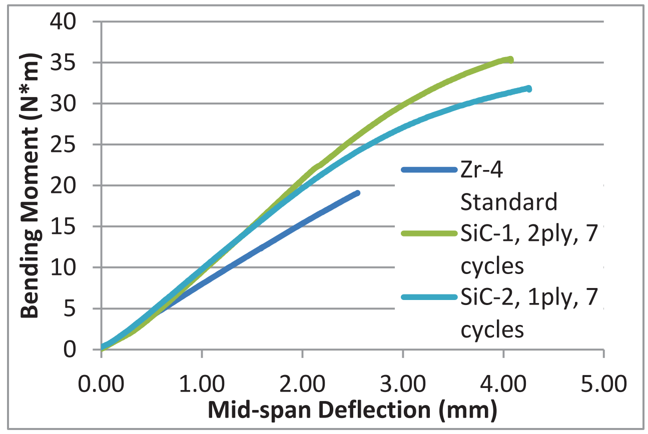

Fig. 5. Bend test results for the mock-up specimens showing bending moment vs mid-span deflection. The 2-ply SiC-CMC hybrid mock-up specimen exhibits the highest bending stiffness, and higher bending resistance.

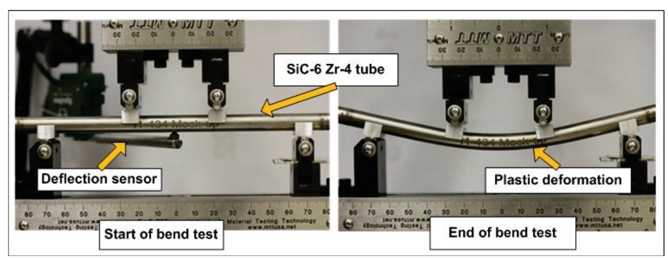

Fig. 6. Bend test results of the Zr-4 mock-up specimen (SiC-6) at the start and end of the bend test (unloaded condition), showing plastic deformation of the specimen that occurred during the test.

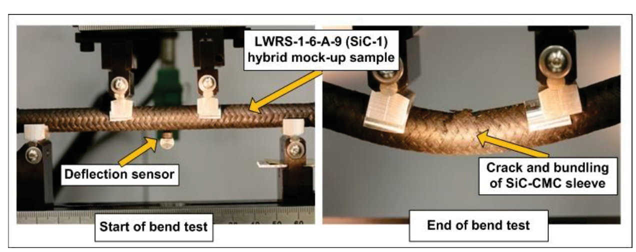

Fig. 7. Bend test results of the 7 cycle, 2-ply LWRS-1-6-A-9 mock-up specimen (SiC-1) at the start and end of the bend test, showing cracking and bundling of the SiC-CMC sleeve on the compressive side of the specimen.

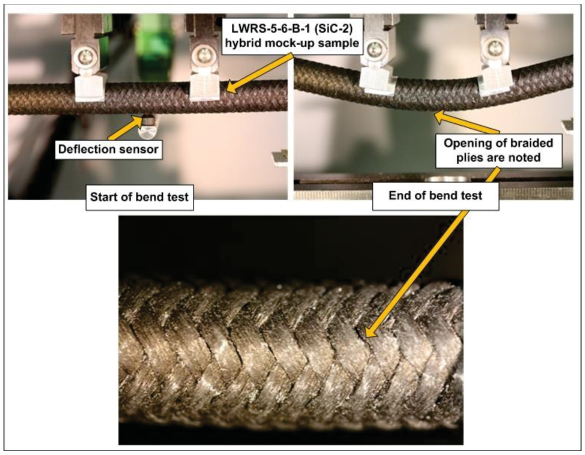

Fig. 8. Bend test results of the 7 cycle, 1-ply LWRS-5-6-B-1mock-up specimen (SiC-2) at the start and end of the bend test, showing the opening of the braided plies. It should be noted that some openings were already visible prior to bend testing.

III.B. SiC-CMC Sleeve Specimens

As mentioned previously, cylindrical support inserts were manufactured to be a close fit to the inside tube diameter for the bend test of the SiC-CMC sleeves. Only sleeves fabricated with 5 PIP cycles were available for these tests, although differentiation could be made between the numbers of braided plies. A 1-ply sleeve, LWRS-1-6-A-3-4, was tested first using half of the displacement rate used for the hybrid mock-up specimens (0.25 mm/min). This rate was selected due to the expected brittle nature of the SiC-CMC sleeve without the ductile Zr-4 tube supporting the sleeve. A validation test on a replicate 1-ply braided sleeve was performed with the displacement rate decreased to 0.15 mm/min. Bend test results of the 5 cycle, 1-ply (LWRS-1-6-A-3-4 and LWRS-1-6-A-6) and the 5 cycles, 2-ply (LWRS-1-6-A-2-3) SiC-CMC sleeves show the higher bending moment of the 2-ply SiC-CMC (Fig. 9). Fig. 10 to 12 show the bend test at the start and completion of all three mock-up specimens. Cracks in the SiC-CMC sleeves are observed for the two sleeves tested at the lower displacement rate: the 1-ply (LWRS-1-6-A-6) and the 2-ply (LWRS-1-6-A-2-3). No cracking was visually noted on the 1-ply LWRS-1-6-A-3-4 sleeve although loosening of the braided weaves was noted.

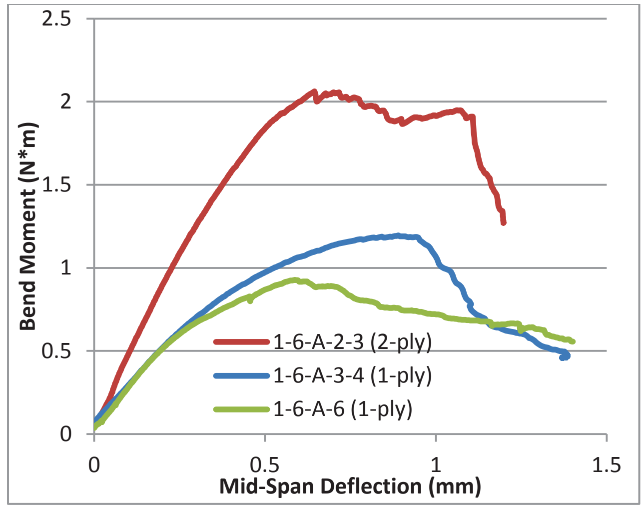

Fig. 9. Bend test results of the two identically fabricated 5 cycle, 1-ply (LWRS-1-6-A-3-4 and LWRS-1-6-A-6) in comparison with the 5 cycle, 2-ply (LWRS-1-6-A-2-3) SiC-CMC sleeves, showing the higher bend moment of the 2-ply SiC-CMC. Tests were stopped and specimens unloaded after substantial load drop where no subsequent bending resistance increase was likely.

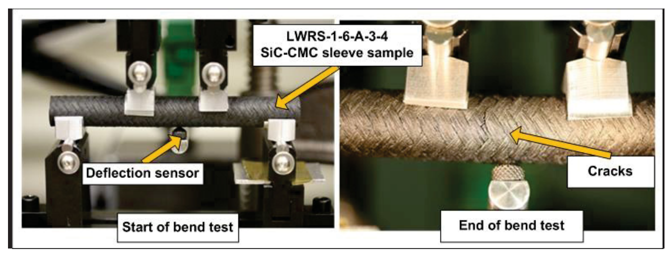

Fig. 10. Bend test results of the 5 cycle, 1-ply LWRS-1-6-A-3-4 SiC-CMC sleeve specimen at the start and end of the bend test, showing cracks.

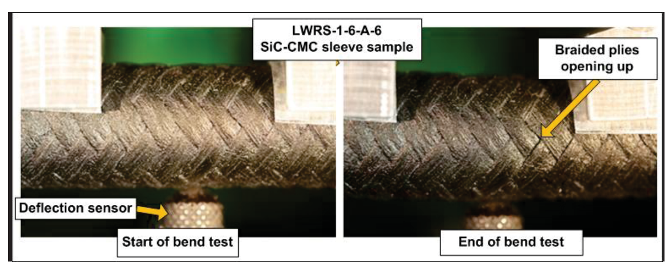

Fig. 11. Bend test results of the 5 cycle, 1-ply LWRS-1-6-A-6 SiC-CMC sleeve specimen at the start and end of the bend test showing no fiber cracks, but “loosening” of the weave pattern suggests that the plies are opening up.

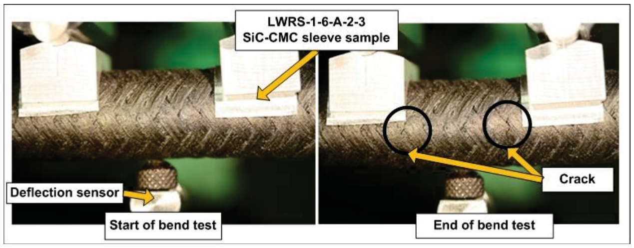

Fig. 12 Bend test results of the 5 cycle, 2-ply (LWRS-1-6-A-2-3) SiC-CMC sleeve specimen at the start and end of the bend test, showing cracks in the mid-span section.

IV. CHARACTERIZATION OF BEND TEST SPECIMENS

The bend test samples were characterized using 3D X-ray tomography and scanning electron microscopy (SEM).

IV.A. Radiographic Examination

Fig. 13 shows a typical example of the deformation of the Zr-4 tube due to the bend test. It is observed that the inner Zr-4 tube of the SiC-1 specimen showed more plastic deformation than other specimens. It is recommended that these results be integrated in future modeling of the hybrid tubes as this typically will show the actual constraints that the SiC-CMC sleeve placed on the inner Zr-4 tube. Please take note that the two micrographs of SiC-6 and SiC-1 cannot be directly compared in this study, as they were not loaded equivalently due to the method alteration needed after testing SiC-6. Comparison will be possible in future tests as the method can now be standardized.

The 3D tomography images (Fig. 14) show the effect that the distortions have on the SiC-CMC-Zr-4 gap at any position. This again may provide design inputs to the simulation codes for the cladding design and needs to be evaluated further in conjunction with the modeling experts. Open porosity was detected in the 1-ply hybrid mock-up specimen (SiC-2) even with the naked eye prior to the bend test (Fig. 15). Additionally 3 D tomography examinations also detected open porosity in the two 1-ply SiC-CMC sleeve specimens (LWRS-1-6-A-3-4and LWRS-1-6-A-6) prior to bend testing (Fig. 16). No open porosity was observed for the 2-ply SiC-CMC sleeve specimen (LWRS-1-6-A-2-3) during the radiographic and visual inspections. The cracks due to the bend test on the three SiC sleeve specimens are shown in Fig. 17 to 19. It is interesting to note that the 2-ply sleeve showed two (almost) parallel cracks but the 1-ply specimens showed one set of cracks branching.

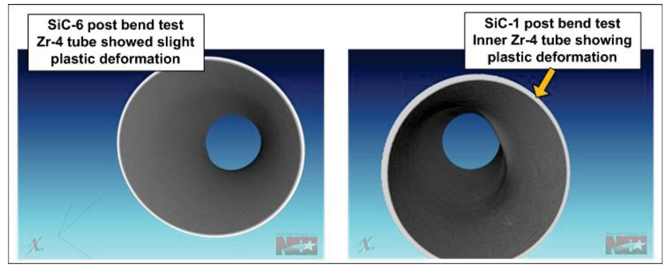

Fig. 13. Post bend test tomography results showing amount of plastic deformation on the inner Zr-4 tube.

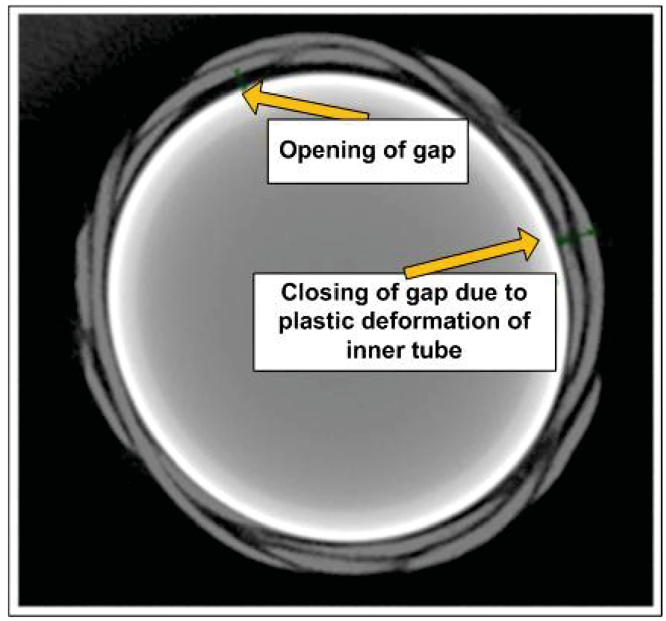

Fig. 14. Post bend test tomography results of hybrid mock-up specimen SiC-2 showing the bending of the inner Zr-4 tube and the subsequent closing of the gap between the SiC-CMC sleeve and the Zr-4 tube.

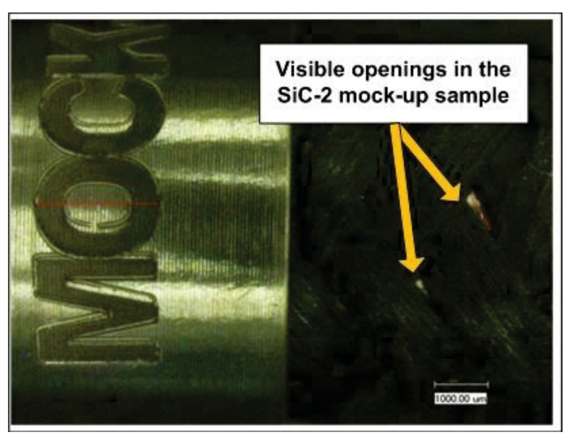

Fig. 15. Visible open porosity in the SiC-2 mock-up specimen (1-ply) prior to radiographic inspection.

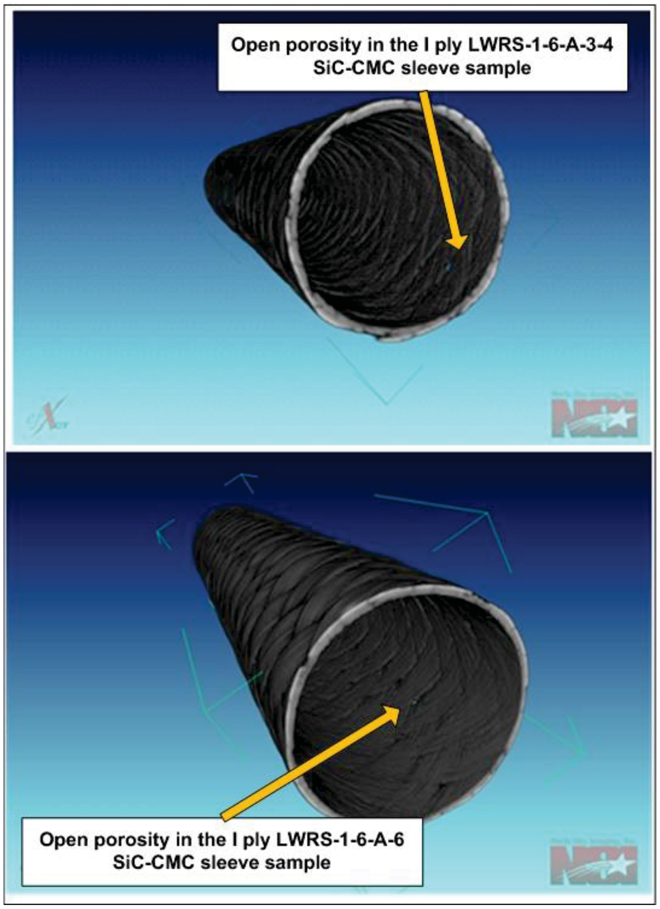

Fig. 16. Open porosity detected in the two 1-ply sleeve specimens (LWRS-1-6-A-3-4 and LWRS-1-6-A-6) during tomography examination.

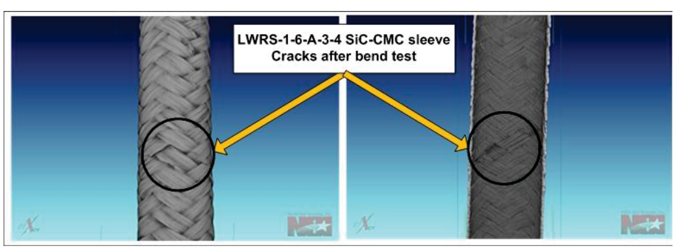

Fig. 17. Post bend test 3D tomography results for the 5 cycle, 1-ply (LWRS-1-6-A-3-4) SiC-CMC sleeve specimen showing cracks.

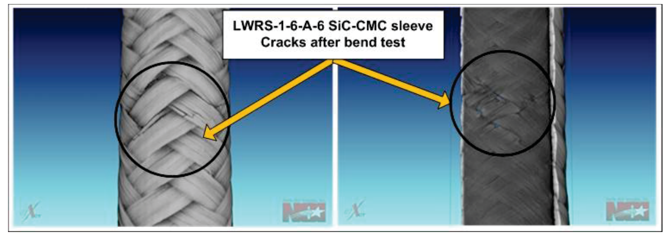

Fig. 18. Post bend test 3D tomography results of the 5 cycle, 1-ply (LWRS-1-6-A-6) SiC-CMC sleeve specimen showing cracks.

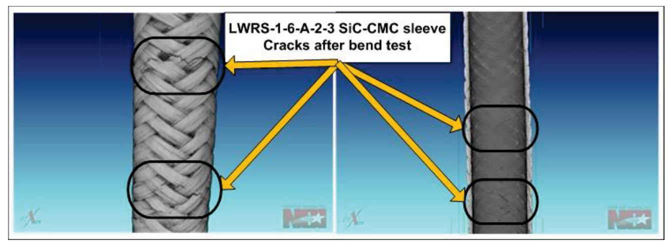

Fig. 19. Post bend test 3D tomography results of the 5 cycle, 2-ply (LWRS-1-6-A-2-3) SiC-CMC sleeve specimen showing two sets of cracks.

IV.B. Metallurgical Examination

A metallurgical examination was completed on the crack regions and at the Zr-4 protection sleeve interface with the SiC-CMC sleeve to establish any adverse effects due to the bend testing. A significant difference in microstructure is observed when comparing the 1- and 2-ply hybrid mock-up specimens, as shown in Fig. 20. The 1-ply SiC-CMC sleeve matrix shows signs of distress and preliminary signs of defraying at these areas, especially at the braided seam. The microstructure of the 2-ply SiC-CMC sleeve appears intact at the end of the protective Zr-4 sleeve and SiC-CMC sleeve interface. This defraying tendency is also notable on examination of the fracture areas. The SiC-CMC matrix material of the 1-ply sleeve shows significant cracking and has a flaky appearance, while the 2-ply matrix material was still bonded together, except at the areas where the actual fracture took place (Fig. 21).

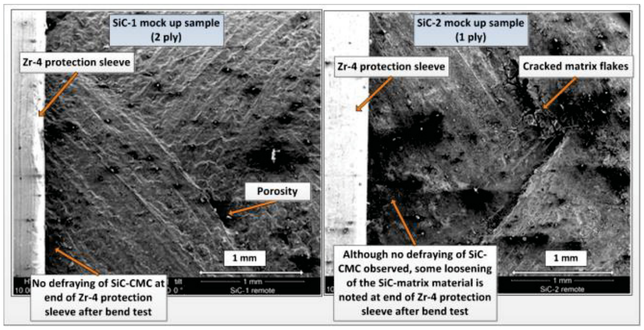

Fig. 20. Difference between integrity of the sleeve at the end caps: 2-ply still intact, 1-ply shows signs of failure and modifications.

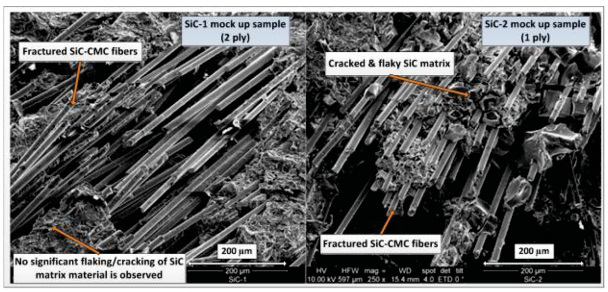

Fig. 21. The CMC fiber fracture morphology of the 1- and 2-ply SiC-CMC mock up specimens appears to be similar. Differences are noted on the SiC matrix material as it appears to be more cracked and flaky in the 1-ply SiC-CMC sleeve compared to the more compact SiC-matrix material of the 2-ply SiC-CMC sleeve.

IV. CONCLUSIONS

The four-point bend tests provided a successful comparison of the mechanical response of various SiC sleeve and tube-sleeve combination specimens. The 2-ply sleeve specimens show a higher resisting bend moment (higher bending stiffness) compared to those of the 1-ply sleeve specimens, as was expected. This is true for both the hybrid mock-up and SiC-CMC "sleeve only" specimens. As expected, the 1- and 2-ply hybrid mock-up specimens had higher bending stiffness (higher bend momentum) if compared to the bare Zr-4 tube specimen.

The characterization of the hybrid mock-up specimens showed that the 1-ply SiC-CMC sleeve matrix shows signs of distress and preliminary signs of fraying at the protective Zr-4 sleeve areas. In addition, the microstructure of the SiC matrix at the cracks after bend test shows significant cracking and flaking. The 2-ply SiC-CMC sleeve specimens showed, however, a more bonded cohesive SiC matrix structure. The cracking and fraying shows potential concerns for increased fretting during the actual use of the SiC-CMC sleeves.

Tomography was proven as a successful tool to identify open porosity during pre-test characterization. Additionally, the benefit of tomography as an indirect tool for establishing simulation parameters was identified and is recommended for further exploration. Additionally, it is further recommended that electron backscatter diffraction (EBSD) is investigated to determine the feasibility and value as a deformation indicator on the Zr-4 tubes. Deformation modes are not known under these conditions for tubular samples, nor are the influence of an external clad on these deformation modes. It is also recommended that future work includes the consideration of compression tests in conjunction with bend testing of clad designs.

ACKNOWLEDGEMENTS

This work was supported by the U.S. Department of Energy, Office of Nuclear Energy, under DOE Idaho Operations Office Contract DE-AC07-05ID14517. Amber Miller and Todd Morris are acknowledged for their contribution towards the bend test characterization measurements. Fred Lauten from Physical Sciences Inc. is acknowledged for the SiC-CMC sleeve fabrication. Michael Teague and Kristine Barrett are acknowledged for the bend test mock-up specimen fabrication.

REFERENCES

1. S.M. Bragg-Sitton, LWRS Fuel Development Plan, INL/MIS-12-25696, Rev.1, December 2012.
2. R. L. Williamson, J.D. Hales, S.R. Novascone, M.R. Tonks, D.R. Gaston, C.J. Permann, D. Andrs, R.C. Martineau, "Multidimensional Multiphysics Simulation of Nuclear Fuel Behavior," Journal of Nuclear Materials, Vol. 423, pp. 149-163, 2012..
3. I.J. van Rooyen, Pre-IrradiationTesting and Analysis to Support the LWRS Hybrid SiC-CMC-Zircaloy-4 Unfueled Rodlet Irradiation, INL/EXT-12-27189, January 2013.